Sulfur Trifluoride Cation (SF_3^+) Affinities of Pyridines Determined by the Kinetic Method: Stereoelectronic Effects in the Gas Phase

Philip S. H. Wong, Shuguang Ma, Sheng Sheng Yang, and R. Graham Cooks

Department of Chemistry, Purdue University, West Lafayette, Indiana, USA

Fabio C. Gozzo and Marcos N. Eberlin

State University of Campinas—UNICAMP, Institute of Chemistry, Campinas, SP, Brazil

Ion/molecule reactions performed by pentaquadrupole mass spectrometry are used to generate cluster ions in which neutral pyridines are bound to the polyatomic cation SF_3^+. The dimeric ions $Py_1SF_3^+Py_2$, where Py_1 and Py_2 represent substituted pyridines, are shown to have loosely bound structures by collision-induced dissociation (MS^3) experiments and by semiempirical AM1 and ab initio RHF/6-31G(*d*, *p*) molecular orbital calculations. In the case of dimers comprised of meta- and/or para-substituted pyridines (unhindered pyridines), there is an excellent linear correlation between the logarithm of the fragment ion abundance ratio $\ln\{[Py_1(SF_3^+)]/[Py(SF_3^+)]\}$ and the proton affinities (PA) of the constituent pyridines. Semiempirical calculations are used to estimate the SF_3^+ affinities of pyridines which are found to be in the range of 25–31 kcal/mol. The SF_3^+ affinities show an excellent linear correlation with the proton affinities of the pyridines, and the relationship SF_3^+ affinity (kcal/mol) = 0.73PA − 135.8 between the two affinities is derived. The effective temperature of the dimeric ions is determined to be 595 ± 69 K, which is in good agreement with values of around 600 K obtained experimentally in studies on many other systems activated under similar conditions. Ortho-substituted pyridines show lower than expected affinities due to stereoelectronic effects that decrease the cation affinities. Gas-phase stereoelectronic parameters (S^k) are measured from the deviation from the PA correlation and are ordered as 2-MePy (−1.09) < 2,6-diMePy (−1.11) < 2-EtPy (−1.91) < 2,3-diMePy (−2.15) < 2,5-diMePy (−2.25) < 2,4-diMePy (−2.40). Overall, the steric effects are larger than those in the corresponding Cl^+-bound dimers but smaller than those in the bulky [$OCNCO^+$] system. Calculations show evidence for agostic bonding that offsets the steric effects in some cases. The eclipsed conformation of 2-methylpyridine/SF_3^+ adduct is found to be more stable than the staggered form by 0.8 kcal/mol, due to auxiliary agostic bonding between the hydrogen of the ortho methyl substituent and the sulfur atom. Calculations on atomic charge distribution reveal that the positive charge is mainly on the sulfur atom (+1.99) and the charge on the bonding hydrogen S–H–C (+0.07) is considerably lower than that on the other two methyl hydrogens (+0.14), which appears to be a good indication of agostic binding. The most stable form of the 2-ethylpyridine/SF_3^+ adduct is found when the $N–C_1–C_\alpha–C_\beta$ dihedral angle is approximately 60°, where the ethyl hydrogen is directed toward the SF_3 group via an interesting six-membered ring alignment. The experiments show a remarkably small steric effect in 2,6-dimethylpyridine, probably due to strong agostic bonding enhanced by the buttressing effect that shortens the S–H distance. In addition, the face-to-face interactions of the F atoms and the H atoms further stabilize this form. © *1997 American Society for Mass Spectrometry (J Am Soc Mass Spectrom 1997, 8, 68–75)*

The solvent and counterion usually have significant effects on reaction kinetics and dynamics in the case of ionic reactions occurring in solution. On the other hand, ion/molecule reactions in the gas phase yield a wealth of kinetic, thermochemical, and structural information in a more direct fashion [1]. The present study of SF_n^+ ions continues a series of investigations into the thermochemistry of electron-deficient ions. Like the earlier studies, the present study employs the kinetic method [2], applied to a cluster ion, a cation-bound dimer. The rates of competitive dissocia-

Address reprint requests to R. G. Cooks, Department of Chemistry, Brown Laboratory, Purdue University, West Lafayette, IN 47907-1393.

1044-0305/97/$17.00
PII S1044-0305(96)00154-7

Received April 18, 1996
Revised August 8, 1996
Accepted August 8, 1996

tions of the cation-bound dimer to give the individual cationized monomers are used to calculate the cation affinity difference between the two compounds. Previous studies have dealt with the ions Cl^+ [3], CN^+ [4], $OCNCO^+$ [5], and $SiCl_n^+$ [6]. Affinities of substituted pyridines for all these Lewis acids have been ordered and compared to proton affinities. Remarkably, the affinities of the meta- and para-substituted pyridines for each of these cations correlates linearly with the corresponding proton affinities. Ortho-substituted pyridines display steric effects and in the case of $SiCl^+$, a stabilizing electronic interaction involving the ortho methyl substituent(s) that has been recognized to be the result of agostic bonding [6].

Thermochemical data for the fluorides SF_x ($x = 0$–6) have been reviewed [7] and the heat of formation, entropy, bond dissociation energy, and the proton affinity of SF_6 have been determined [8]. However, there is very little information on the chemistry of the cations SF_y^+ ($y = 1$, 3, and 5) [9], even though they have been implanted into GaAs field-effect transistors to improve performance [10].

The goals of this study are (1) to investigate SF_3^+ affinities of a group of alkyl-substituted pyridines, (2) to measure steric effects that might arise for ortho-substituted pyridines, (3) to seek further examples of gas-phase agostic bonding first observed in the $SiCl^+$ case [6], and (4) to investigate cluster ion formation in the cases of SF^+, $SF_2^{+\cdot}$, $SF_4^{+\cdot}$, and SF_5^+. A series of pyridines was chosen for study because they are strong bases in which ring substitutents can be introduced to systematically modify their electronic and steric effects. In addition, a number of cation affinities are being studied to understand the relationship among the cation affinities, including the effects of the size of the cations and the slope of the correlation line of cation with proton affinity.

Experimental

The MS^2 and MS^3 experiments were performed by using a custom-built pentaquadrupole mass spectrometer [11] comprised of three mass-analyzing quadrupoles (Q1, Q3, Q5) and two reaction quadrupoles (Q2, Q4). For MS^2 experiments, SF_3^+ was generated by 70-eV electron ionization of sulfur hexafluoride in the ion source and mass-selected by using Q1. The mass-selected SF_3^+ ion was then allowed to undergo ion/molecule reactions with a mixture of pyridines in Q2. The reaction products were analyzed by scanning Q5 with both Q3 and Q4 set in the broad-band transmission rf-only mode. For MS^3 experiments, particular ion/molecule reaction products formed in Q2 were mass-selected by using Q3 and allowed to undergo energetic collisions with argon in Q4, while Q5 was scanned to record the sequential product ion spectrum, a particular type of MS^3 spectrum [12].

Sulfur hexafluoride gas was introduced into the ion source via a Granville Phillips valve (Granville Phillips Co., Boulder, CO) at a nominal pressure of 4×10^{-6} torr. The indicated pressure rose to 4×10^{-5} torr upon addition of the pyridine mixture to Q2, and further increased to 7×10^{-5} torr upon addition of argon gas to Q4. The attenuation of the ion beam upon introducing the argon collision gas was about 80%. The collision energy—the nominal voltage difference between the ion source and the collision quadrupole—was near 0 eV in Q2 for ion/molecule reactions and 10 eV in Q4 for MS^3 experiments, respectively. The pyridines and sulfur hexafluoride are commercially available and were used as received. Mass-to-charge ratios are reported by using the Thomson unit (Th) [13].

The SF_3^+ affinities of pyridines were estimated by AM1 molecular orbital calculations [14]. AM1 and ab initio calculations were carried out by using Spartan 4.0 (Spartan version 4.0, Wavefunction, Inc., Irvine, CA). A partial ab initio geometry optimization was carried out for the $[Py–SF_3–Py]^+$ dimer. First, the structure was fully optimized by AM1 calculations, followed by ab initio optimization of all geometric parameters except those used only to define the two pyridine rings. No special parameters were used in optimizing the S–N bonds, but the ones already incorporated in AM1 were implemented in Spartan.

Results and Discussion

Figure 1 shows a typical MS^2 ion/molecule reaction product spectrum for reaction of mass-selected SF_3^+ (89 Th) with a mixture of 4-methylpyridine (4-MePy) and pyridine (Py). The spectrum shows that there are two major types of products: the H^+-bound clusters and SF_3^+-bound clusters of pyridines. In the case of the H^+-bound clusters, the protonated pyridines (80 and 94 Th) and the proton-bound dimers (159, 173, and 187 Th) probably arise via charge exchange of a pyridine with the SF_3^+ ion, and subsequent proton transfer and association reactions. In the case of the SF_3^+-bound clusters, the SF_3^+ ion forms 1:1 adducts (168 and 182 Th) and 1:2 adduct (247, 261, and 275 Th) with the neutral pyridines.

When the unsymmetrical SF_3^+-bound dimer (261 Th) is mass-selected in Q3 and fragmented by collision-induced dissociation (CID) with argon in the second reaction region (Q4) under mild conditions (collision energy 10 eV), the only fragments observed are the two monoadducts $PySF_3^+$ (168 Th) and $4\text{-}MePySF_3^+$ (182 Th) as shown in Figure 2. This result, and the gentle activation conditions under which it is obtained [3], indicate that the dimers of interest are loosely bound. The independence of the spectrum on the relative pressures of the two pyridines indicates a symmetrical, loosely bound structure as is also evident from ab initio molecular orbital calculations (Figure 3). The SF_3^+ dimers are therefore analogous to the dimers encountered in earlier studies on Cl^+ and $OCNCO^+$ [3, 5]. In addition, the AM1 calculations show that SF_3^+ addition to pyridine leads to a stable adduct when

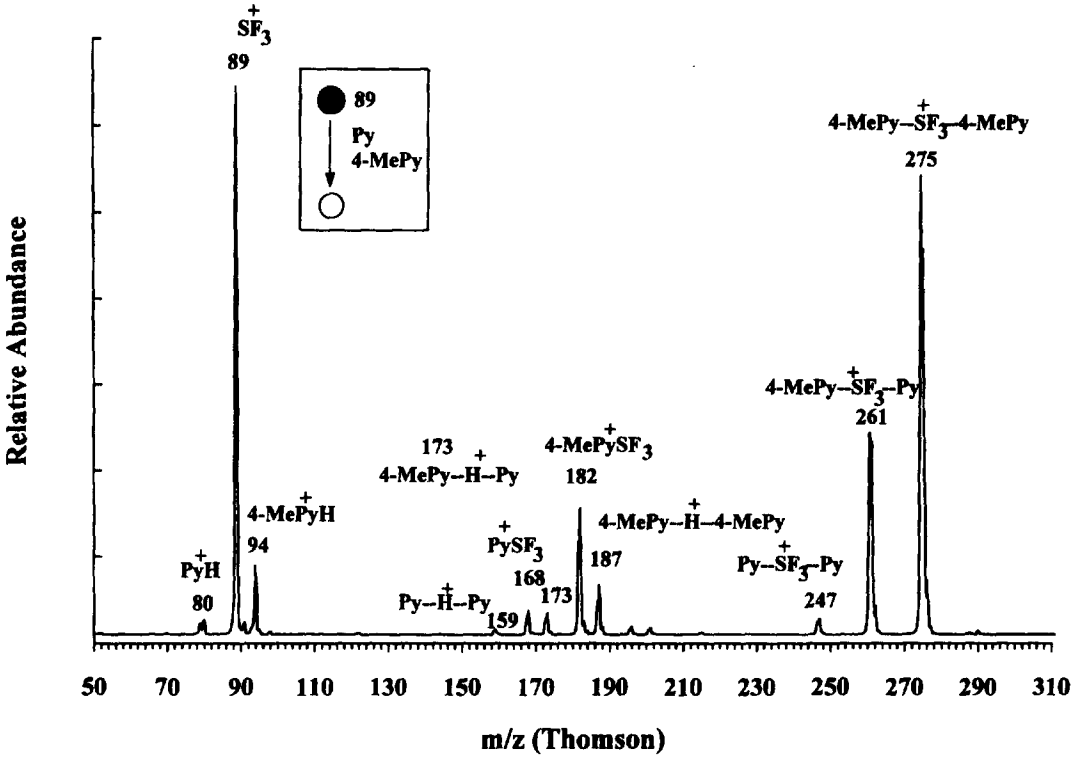

Figure 1. MS^2 product spectrum displaying products of ion/molecule reactions of mass-selected SF_3^+ (89 Th) ions with a mixture of pyridine (Py) and 4-methylpyridine (4-MePy).

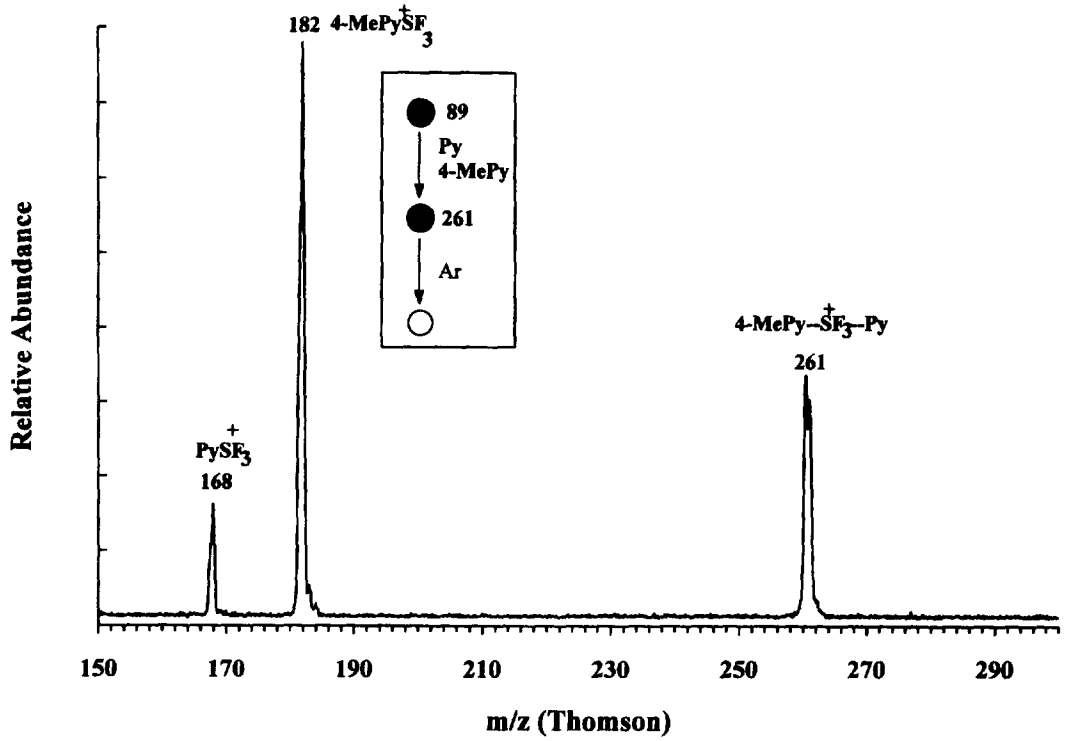

Figure 2. MS^3 sequential product spectrum showing fragmentation of the mixed dimeric adduct (261 Th) generated upon reaction of SF_3^+ with a mixture of pyridine (Py) and 4-methylpyridine (4-MePy).

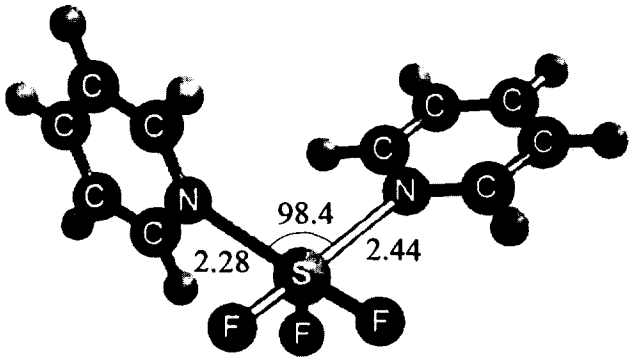

Figure 3. Structure of the lowest energy, loosely bound form of the $Py[SF_3^+]Py$ dimer optimized by ab initio molecular orbital calculations. A partial optimization has been carried out; see text. Bond lengths are in angstroms. Low energy isomerism interconverts the two N–S bonds.

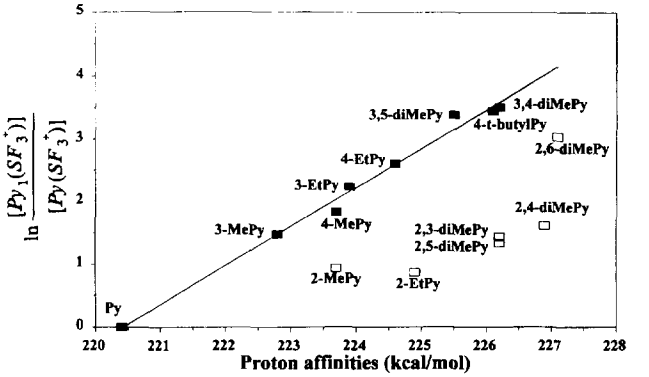

Figure 4. Linear correlation between $\ln\{[Py_1(SF_3^+)]/[Py(SF_3^+)]\}$, which is proportional to the relative SF_3^+ affinities of substituted pyridines, and the corresponding proton affinities. Open symbols represent ortho-substituted pyridines that do not correlate due to stereoelectronic effects.

addition occurs at the ring nitrogen, while the loosely bound dimer is considerably more stable thermodynamically than the two most likely covalently bond dimers (Scheme I).

If entropy effects cancel [2] in the competitive fragmentation of loosely bound dimers, the two monomers should be formed in relative abundances that are related to the difference in the SF_3^+ affinities of the two pyridines:

$$\ln \frac{[Py_1SF_3^+]}{[Py_2SF_3^+]} = \frac{\Delta(SF_3^+ \text{ affinity})}{RT_{\text{eff}}} \qquad (1)$$

where R is the gas constant, T_{eff} is the effective temperature of the dissociating cluster ion, and the terms in square brackets are product ion abundances. The use of this relationship is limited by the lack of independently known SF_3^+ affinity values and the difficulty of measuring the effective temperature of the activated dimer. However, relative SF_3^+ affinities can be ordered and, if the same electronic effects that influence proton affinities also affect SF_3^+ affinities, a linear relationship should exist between $\ln\{[Py_1(SF_3^+)]/[Py(SF_3^+)]\}$ and the proton affinities. That this is the case for the unhindered pyridines is evident from the data shown in Figure 4. The existence of the linear correlation confirms that the dimers are symmetrically bound with respect to the central sulfur atom; otherwise the order of pyridine addition to the cation would affect the ease of dissociation. This structural assignment has been confirmed by ab initio calculations in the analogous case of Cl^+, CN^+, and $OCNCO^+$ cations [3–5].

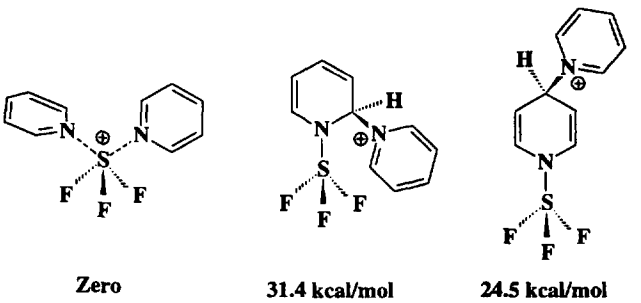

Scheme I. Relative stabilities of the three alternative structures for $(Py)_2SF_3^+$ dimers calculated by AM1 (kilocalories per mole).

The SF_3^+ affinities of pyridines were estimated by AM1 molecular orbital calculations and the results are summarized in Table 1. Although the errors in the AM1 calculation of the absolute affinities are unknown, only relative values for a series of closely related compounds are of interest, so much of the error is likely to cancel. Figure 5 shows a plot of $\ln\{[Py_1(SF_3^+)]/[Py(SF_3^+)]\}$ versus AM1 SF_3^+ affinities. According to eq 1, the slope of this line should be equal to $1/RT_{\text{eff}}$, and therefore T_{eff} is found to be 595 ± 69 K. This temperature is in good agreement with values of around 600 K obtained experimentally in studies [15, 16] on many other systems activated under similar conditions. The AM1-determined effective temperature of 595 K and the calculated value for the SF_3^+ affinity for pyridine (25.8 kcal/mol) can be used in combination with the experimental $\ln\{[Py_1(SF_3^+)]/[Py(SF_3^+)]\}$ values to calculate the absolute SF_3^+ affinities of the other pyridines by using eq 1; the results are collected in Table 1. The absolute SF_3^+ affinities of the meta- and para-substituted pyridines are in excellent agreement with the AM1 SF_3^+ affinities. The decreases caused by the steric effects of ortho group(s) are taken into account in the experimental results, even though these effects were poorly estimated by the AM1 method. The absolute values of SF_3^+ affinities (kcal/mol) correlate with the proton affinities of the unhindered pyridines by the equation

$$SF_3^+ \text{ affinity} = 0.73PA - 135.8 \qquad (2)$$

with a correlation coefficient $r^2 = 0.9886$. In the cases of the cations $OCNCO^+$, $SiCl_3^+$, Cl^+, CN^+, and $SiCl^+$, the slopes of the equations analogous to eq 2 were 0.96, 0.95, 0.83, 0.72, and 0.60, respectively [3–6]. Note that an effective temperature of 555 K was assumed in

Table 1. SF_3^+ affinities and proton affinities of pyridines

Entry	Pyridines	Py_1:Py_2[c]	$\ln\left\{\frac{[Py_1(SF_3^+)]}{[Py(SF_3^+)]}\right\}$[d]	Proton affinity[a] (kcal/mol)	AM1 SF_3^+ affinity (kcal/mol)	Absolute SF_3^+ affinity[b] (kcal/mol)
1	Py		0	220.4	25.8	25.8
2	3-MePy	2:1	1.48	222.8	27.8	27.5
3	4-MePy	3:1	1.83	223.7	28.3	28.0
4	3-EtPy	4:2	2.24	223.9	28.0	28.4
5	4-EtPy	5:2	2.61	224.6	29.1	28.9
6	3,5-diMePy	6:3	3.39	225.5	29.0	29.8
7	4-*t*-butylPy	7:3	3.45	226.1	30.0	29.9
8	3,4-diMePy	8:3	3.51	226.2	30.0	29.9
9	2-EtPy	9:3	0.87	224.9	30.5[e]	26.8
10	2MePy	10:1	0.94	223.7	28.4[e]	26.9
11	2,5-diMePy	11:3	1.34	226.2	29.6[e]	27.4
12	2,3-diMePy	12:3	1.44	226.2	29.5[e]	27.5
13	2,4-diMePy	13:3	1.62	226.9	30.6[e]	27.7
14	2,6-diMePy	14:3	3.04	227.1	29.3[e]	29.5

[a] Proton affinities are taken from Aue, D. H.; Bowers, M. T. In *Gas Phase Ion Chemistry*; Bowers, M. T., Ed.; Academic: New York, 1979, Vol. 2. This older set of values is used in preference to others because it is internally more consistent and it facilitates comparison of the present data with those for pyridine binding to other cations. See ref 6 for a discussion of this point.

[b] The absolute SF_3^+ affinities were obtained by applying eq 1 and using experimental and theoretical results; that is, the experimental values of $\ln\{[Py_1(SF_3^+)]/[Py(SF_3^+)]\}$, T_{eff} extracted from the plot shown in Figure 5, and the AM1 SF_3^+ affinity value of pyridine.

[c] The entry number of the pyridine forming the SF_3^+-bound dimer used to estimate the SF_3^+ affinity.

[d] Experimental results.

[e] The affinity value is calculated based on the most stable conformation.

these cases. The slope of the correlation line is expected to reflect the relative cation–ligand bond strength [17]. The small slope of 0.73 in the current case of SF_3^+ suggests that there is somewhat weaker bonding between SF_3^+ and pyridine. The calculated SF_3^+ affinity values in the range of 25–31 kcal/mol (see Table 1) also indicate the weakness of the SF_3^+-pyridine bond. As a result of weaker bonding, the bond length Py-SF_3^+ (N–S) is expected to be relatively long. As shown in Figure 3, ab initio calculations for the Py–SF_3^+–Py dimer display an average S–N bond length of 2.36 Å. The calculations also show that the two pyridine rings are perpendicular in the dimer, a geometry which minimizes steric interference between the two pyridines and that leads to slightly different S–N bond lengths.

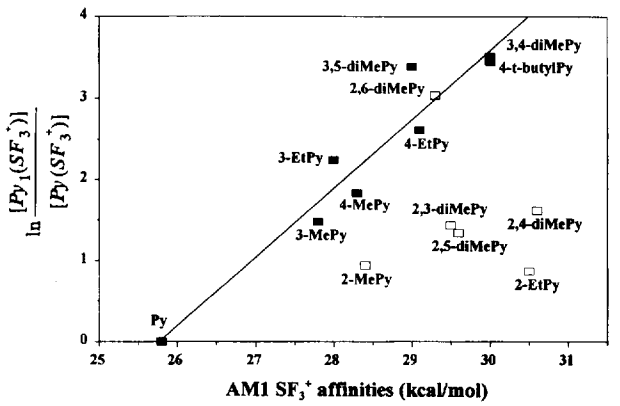

Figure 5. Linear correlation between $\ln\{[Py_1(SF_3^+)]/[Py(SF_3^+)]\}$ and the corresponding calculated AM1 SF_3^+ affinities for unhindered pyridines (filled square). Ortho-substituted pyridines (open square) do not correlate.

It has been shown previously that the presence of an alkyl substituent at the ortho position of a pyridine lowers the Cl^+, CN^+, $OCNCO^+$, and $SiCl_3^+$ cation affinities [3–6]. This was attributed to steric hindrance due to the alkyl group. A measure of this effect—S^k, a gas-phase stereoelectronic parameter—is given by the deviation of the experimentally measured logarithm of the ion abundance ratio from the linear regression line [3, 18]. As shown in Figure 4, the correlation of the logarithm of the ion abundance ratio with proton affinity is generally excellent for meta- and para-substituted pyridines, but poor for the ortho-substituted compounds. The gas-phase stereoelectronic parameters S^k are ordered as 2-MePy (−1.09) < 2,6-diMePy (−1.11) < 2-EtPy (−1.91) < 2,3-diMePy (−2.15) < 2,5-diMePy (−2.25) < 2,4-diMePy (−2.41), and are listed in Table 2.

Although the S^k values do show significant steric hindrance between the ortho substituents and the SF_3 group, additional binding that mitigates this effect is indicated by the calculations. For instance, if one considers only steric hindrance effects, the staggered form (b) (Figure 6) of the 2-methylpyridine/SF_3^+ adduct would be expected to be significantly more stable than

Table 2. Steric parameters for ortho-substituted pyridines in SF_3^+-bound dimers and other cation-bound dimers

Pyridine	$\ln([Py_1(SF_3^+)]/[Py_2(SF_3^+)])$		S^k			
	Experimental	Calculated[a]	SF_3^+[b]	$OCNCO^+$[c]	Cl^+[d]	$SiCl_3^+$[e]
Py	0	0	0	0	0	0
2-EtPy	0.87	2.78	−1.91	—	—	—
2MePy	0.94	2.03	−1.09	−1.39	−0.43	−0.47
2,5-diMePy	1.34	3.59	−2.25	−3.02	—	−0.32
2,3-diMePy	1.44	3.59	−2.15	−3.29	−0.64	−0.22
2,4-diMePy	1.62	4.02	−2.40	−3.15	—	−0.71
2,6-diMePy	3.04	4.15	−1.11	−5.09	−1.6	−0.94

[a] Calculated data from linear regression equation of the line in Figure 4.
[b] S^k value is the difference between the experimental data and the calculated data.
[c] S^k value is taken from ref 5.
[d] S^k value is taken from ref 3.
[e] S^k value is taken from ref 6.

the eclipsed form (a), an effect that should be enhanced by the bulky SF_3 group. However, AM1 calculations show that conformer (a) (Figure 6) is 0.8 kcal/mol more stable than the staggered conformer (b). Actually the energy of the staggered form (b) could only be calculated via a constrained optimization, since this form was found to be unstable and to collapse to the most stable form (a) without any appreciable barrier during an unconstrained geometry optimization procedure. Note that in the eclipsed form (a), the SF_3 group adopts an interesting geometry that better exposes the sulfur atom allowing a more efficient interaction with the hydrogen, while in form (b) SF_3 is essentially tetrahedral. This extra interaction—auxiliary binding—explains why the eclipsed form is more stable than the staggered form. This kind of auxiliary binding is quite similar to solution phase agostic bonding [19–22], which is a form of three-center two-electron bonding (M–H–C) in which the two electrons in the C–H bond are formally donated to the metal center M. It is interesting that ab initio linear combination of atomic orbitals–self-consistent field–molecular orbital LCAO-SCF-MO calculations were used to provide the first theoretical evidence for an agostic M–H–C interaction [23]. Scheme II shows charge distributions in the eclipsed conformation. The positive charge is mainly on the sulfur atom (+1.99), which should very much favor agostic bonding because of the greater electron affinity of the S atom. On the other hand, the charge on the bonding hydrogen S–H–C (+0.07) is considerable lower than that of the other two hydrogens (+0.14), which appears to be a good indication of auxiliary bonding.

The case of 2-ethylpyridine is also very interesting. There are two minima and the most stable one is seen when the $N–C_1–C_\alpha–C_\beta$ dihedral angle is approximately 60° (Figure 7; SF_3^+ affinity = 30.5 kcal/mol). The second most stable form is observed for a dihedral angle of 90° (affinity = 28.9 kcal/mol) and the energy maximum (lowest affinity) is obtained at 180° (affinity = 27.1 kcal/mol). Again, if there is no auxiliary binding, the most stable form shown in Figure 7 would be the most energetic one due to severe hindrance between the methyl group and the SF_3 group. Note that in the 60° conformation, the ethyl hydrogen is directed toward the SF_3 group via an interesting

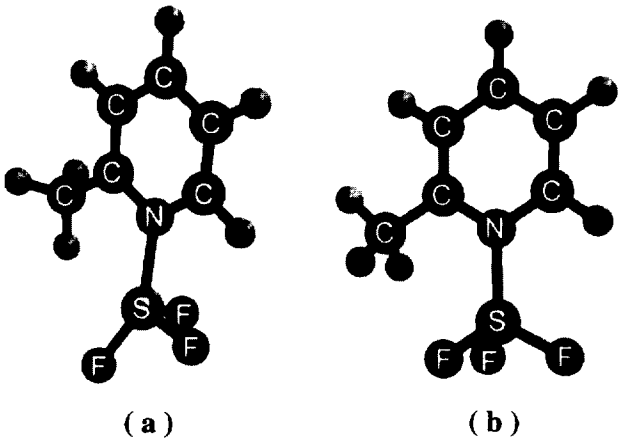

Figure 6. AM1-optimized structures of (a) eclipsed conformer (ΔH_f = 21.3 kcal/mol) and (b) staggered conformer (ΔH_f = 22.1 kcal/mol) of the adduct 2-methylpyridine/SF_3^+. The lower energy of (a) is evidence for agostic bonding. Note also that in form (a) the SF_3 group adopts an interesting geometry that exposes the sulfur atom for more efficient interaction with the hydrogen atom of the methyl group, while in form (b) it is essentially tetrahedral.

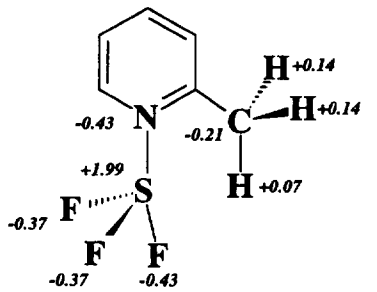

Scheme II. Charge distribution of the eclipsed conformation of the adduct 2-methylpyridine/SF_3^+.

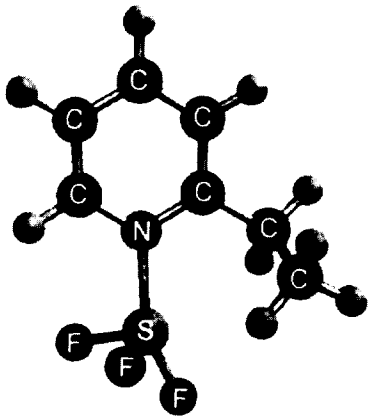

Figure 7. The most stable form of the 2-ethylpyridine/SF_3^+ adduct obtained by AM1 geometry optimization. Note the six-membered ring alignment that allows for additional binding between sulfur and the methyl hydrogen.

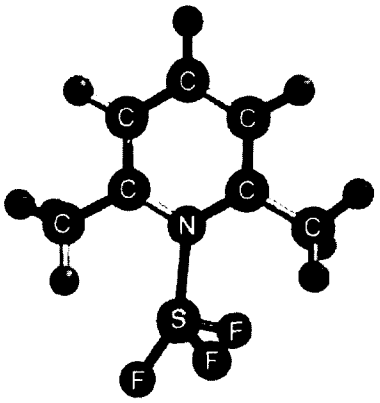

Figure 8. AM1-optimized structure of the most stable conformation of the adduct 2,6-dimethylpyridine/SF_3^+. Note that one methyl group assumes an eclipsed form, while the other is staggered with relation to SF_3, as expected considering the operation of either agostic bonding and steric hindrance. The buttressing effect of the staggered ortho methyl group enhances the S–H agostic binding and the face-to-face orientation of the two F and H atoms of the staggered ortho methyl group may allow for some additional binding.

six-membered ring alignment. Although the differences in the energies of the various conformers are not large and significant interconversion might occur at 600 K, the most stable conformation should still have a significant effect on the properties of the ion. The fact that the calculations rationalize the experimental data supports this contention.

Yet another interesting case is provided by the 2,6-dimethylpyridine/SF_3^+ adduct. Steric effects should be the largest in this pyridine due to the two ortho methyl substituents, and this result is observed for the Cl^+ [3], $[OCNCO]^+$ [5], and $SiCl_3^+$ [6] pyridine adducts. For SF_3^+, however, the stereoelectronic parameter S^k is quite small (Table 2). This is probably due to a relatively stronger agostic bonding with an ortho methyl group enhanced by the buttressing effect of the other ortho methyl group, which bends the N–SF_3 bond and shortens the S–H distance. In addition, there might be some additional interactions between the two F atoms and the two H atoms of the staggered methyl substituent as a result of their face-to-face orientations (Figure 8).

The stereoelectronic parameter S^k in the present case therefore arises from a combination of both steric and electronic (agostic) effects. A negative sign of the S^k values for the ortho-substituted pyridines, as found here, indicates that the steric effect is stronger than the agostic effect. In the case of $SiCl^+$ [6], the S^k values had positive signs, indicating the greater strength of the agostic effect. The weak agostic effect observed in the current system is probably due to the large steric bulk of the SF_3 group compared to the SiCl group and the long N–S bond, which results in a large separation between the ortho methyl hydrogen atom and the sulfur atom, thus reducing their through-space interactions. It could also be that the Si–H interaction is intrinsically stronger than S–H.

Comparison between the steric effect for 2-methylpyridine in the Cl^+-bound dimer ($S^k = -0.43$), the $OCNCO^+$-bound dimer ($S^k = -1.39$), the $SiCl_3^+$-bound dimer ($S^k = -0.47$), and the SF_3^+-bound dimer ($S^k = -1.09$) clearly demonstrates that the SF_3^+ system has a larger steric effect than the Cl^+ and $SiCl_3^+$ systems, but one that is smaller than the bulky $[OCNCO]^+$ system (see Table 2). (The occurrence of agostic Si–H–C bonding in the $SiCl^+$ [6] case obscures the steric parameter and prevents comparison with the SF_3^+ system.) The large steric effect in the SF_3^+ system may be due to the fact that the lone pair of electrons on the sulfur atom causes the dimeric ion [Py–SF_3^+–Py] to adopt an approximately square pyramidal structure (Figure 3), which causes more steric crowding when an ortho substituent is present on the pyridine. Ab initio calculations show that the Py-S-Py angle in the dimeric ion is 98.4°.

Ion/molecule reactions of pyridines with SF^+, $SF_2^{+\cdot}$, $SF_4^{+\cdot}$, and SF_5^+ were also investigated. Charge exchange and association reactions are the main reaction channels. For example, ion/molecule reactions of SF^+ with a mixture of pyridine and 3-methylpyridine yield protonated pyridine [PyH^+ (80 Th)], protonated methylpyridine [3-$MePyH^+$ (94 Th)], and proton-bound dimers of pyridine and 3-methylpyridine [Py–H^+–Py (159 Th), Py–H^+–3-MePy (173 Th), 3-MePy–H^+–3-MePy (187 Th)] as the major ions. Minor amounts of SF^+–Py (130 Th) and SF^+–3-MePy (144 Th) were also observed. Similar results were observed in the case of SF_5^+. In the cases of the radical cations $SF_2^{+\cdot}$ and $SF_4^{+\cdot}$, only the protonated pyridines and the proton-bound dimers of pyridines were formed. Attempts to make the pyridine dimer with SCl^+, to compare directly with the $SiCl^+$ case, were unsuccessful; only protonated pyridines and the proton-bound dimers of pyridines were observed.

Conclusions

The SF_3^+ affinities of pyridines are determined and, even though their correlation with proton affinities displays a relatively large slope, their values are found to be relatively smaller than those for other cations such as $OCNCO^+$, $SiCl_3^+$, and Cl^+. This anomaly remains to be explained, although it may be associated in part with the inaccuracy of the absolute SF_3^+ affinity values derived by AM1 calculations.

The SF_3^+ affinities of pyridines containing ortho substituents are affected, in opposing directions, by both steric and agostic effects. The steric effect decreases the cation affinities, while the agostic effect increases the cation affinities through interactions between the sulfur atom and the hydrogen of the ortho-substituted alkyl group(s). The presence of agostic bonding is supported by AM1 and ab initio molecular calculations, and even though there may be considerable error in the former values, rationalization of subtle experimental effects is achieved and the relative trends derived from the calculations seem to be reliable. Agostic bonding through the fluorine atom was considered, but is not supported by the calculations. The calculations also demonstrate that the agostic effect determines the favored conformation of the system, leading in some cases to eclipsed conformations as the most stable structures. The relatively weak agostic effect found here is reasonably associated with the large steric bulk of the SF_3 group and the large N–S bond length in the substituted pyridine/SF_3^+ complex. The recognition of gas-phase agostic bonding is important because the activation of carbon–hydrogen bonds by transition metal systems is likely to proceed via initial coordination of the C–H bond to the metal center [20]. Future work will involve thermochemical studies of agostic bonding in other cationic systems.

Acknowledgments

The work at Purdue was supported by the National Science Foundation (CHE 92-23791) and that at UNICAMP by the Research Support Foundation of the State of São Paulo (PAPESP) and the Brazilian National Research Council (CNPg). P. W. thanks Eli Lilly and Company for fellowship support.

References

1. (a) Bowers, M. T., Ed. *Gas Phase Ion Chemistry*, Vols. 1–3; Academic: New York, 1979; (b) Futrell, J. H., Ed. *Gaseous Ion Chemistry and Mass Spectrometry*; Wiley: New York, 1986; (c) Lias, S. G.; Ausloos, P. *Ion–Molecule Reactions, Their Role in Radiation Chemistry*; American Chemical Society: Washington, DC, 1975; (d) Franklin, J. L., Ed. *Ion–Molecule Reactions*; Plenum: New York, 1972; (e) Harrison, A. G., Ed. *Chemical Ionization Mass Spectrometry*; CRC: Boca Raton, FL, 1983.
2. (a) Cooks, R. G.; Patrick, J. S.; Kotiaho, T.; McLuckey, S. A. *Mass Spectrom. Rev.* **1994,** *13,* 287; (b) McLuckey, S. A.; Cameron, D.; Cooks, R. G. *J. Am. Chem. Soc.* **1981,** *103,* 1313.
3. Eberlin, M. N.; Kotiaho, T.; Shay, B. J.; Yang, S. S.; Cooks, R. G. *J. Am. Chem. Soc.* **1994,** *116,* 2457.
4. Yang, S. S.; Bortolini, O.; Steinmetz, A.; Cooks, R. G. *J. Mass Spectrom.* **1995,** *30,* 184.
5. Yang, S. S.; Chen, G.; Ma, S.; Cooks, R. G.; Gozzo, F. C.; Eberlin, M. N. *J. Mass Spectrom.* **1995,** *30,* 807.
6. Yang, S. S.; Wong, P.; Ma, S.; Cooks, R. G. *J. Am. Soc. Mass Spectrom.* **1996,** *7,* 198.
7. Herron, J. T. *J. Phys. Chem. Ref. Data* **1987,** *16,* 1.
8. (a) Mackay, G. I.; Schiff, H. I.; Bohme, D. K. *Int. J. Mass Spectrom. Ion Processes* **1992,** *117,* 38; (b) Latimer, D. R.; Smith, M. A. *J. Chem. Phys.* **1994,** *101,* 3410.
9. (a) Stone, J. A.; Wytenberg, W. J. *Int. J. Mass Spectrom. Ion Processes* **1989,** *94,* 269; (b) Zangerle, R.; Hansel, A.; Richter, R.; Lindinger, W. *Int. J. Mass Spectrom. Ion Processes* **1993,** *129,* 117; (c) Cheung, Y.-S.; Chen, Y.-J.; Ng, C.-Y.; Chiu, S.-W.; Li, W.-K. *J. Am. Chem. Soc.* **1995,** *117,* 9725; (d) Dillard, J. G.; Troester, J. H. *J. Phys. Chem.* **1975,** *79,* 2455; (e) Fehsenfeld, F. C. *J. Chem. Phys.* **1971,** *54,* 438; (f) Babcock, L. M.; Streit, G. E. *J. Chem. Phys.* **1981,** *75,* 3864.
10. Tamura, A.; Inoue, K.; Onuma, T.; Sato, M. *Appl. Phys. Lett.* **1987,** *51,* 1503.
11. Schwartz, J. C.; Schey, K. L.; Cooks, R. G. *Int. J. Mass Spectrom. Ion Processes* **1990,** *101,* 1.
12. (a) Schwartz, J. C.; Wade, A. P.; Enke, C. G.; Cooks, R. G. *Anal. Chem.* **1990,** *62,* 1809; (b) Cooks, R. G.; Amy, J.; Bier, M.; Schwartz, J. C.; Schey, K. L. *Adv. Mass Spectrom.* **1989,** *11A,* 33; (c) Juliano, V. F.; Gozzo, F. C.; Eberlin, M. N.; Kascheres, C.; Lago, C. L. *Anal. Chem.* **1996,** *68,* 1328.
13. Cooks, R. G.; Rockwood, A. L. *Rapid Commun. Mass Spectrom.* **1991,** *5,* 93.
14. Dewar, M. J. S.; Zoebisch, E. G.; Healy, E. F.; Stewart, J. J. P. *J. Am. Chem. Soc.* **1985,** *107,* 3902.
15. (a) Majumdar, T. K.; Clairet, F.; Tabet, J.-C.; Cooks, R. G. *J. Am. Chem. Soc.* **1992,** *114,* 2897; (b) Ho, Y.; Squires, R. R. *J. Am. Chem. Soc.* **1992,** *114,* 10961.
16. Nourse, B. D.; Cooks, R. G. *Int. J. Mass Spectrom. Ion Processes* **1991,** *106,* 249.
17. (a) Corderman, R. R.; Beauchamp, J. L. *J. Am. Chem. Soc.* **1976,** *98,* 3998; (b) Jones, R. W.; Staley, R. H. *J. Phys. Chem.* **1982,** *86,* 1387; (c) Operti, L.; Tews, E. C.; Freiser, B. S. *J. Am. Chem. Soc.* **1988,** *110,* 3847.
18. Jenkins, H. D. B.; Kelly, E. J.; Samuel, C. J. *Tetrahedron Lett.* **1994,** *34,* 6543.
19. Brookhart, M.; Green, M. L. H. *J. Organomet. Chem.* **1983,** *250,* 395.
20. (a) Green, M. L. H. *Pure Appl. Chem.* **1984,** *56,* 47; (b) Brookhart, M.; Green, M. L. H.; Wong, L-L. In *Progress in Inorganic Chemistry*; Lippard, S. J., Ed.; Wiley: New York, 1988; Vol. 36, p 1.
21. Crabtree, R. H.; Holt, E. M.; Lavin, M.; Morehouse, S. M. *Inorg. Chem.* **1985,** *24,* 1986.
22. Carmona, E.; Contreras, L.; Poveda, M. L.; Sànchez, J. *J. Am. Chem. Soc.* **1991,** *113,* 4322.
23. Koga, N.; Obara, S.; Morokuma, K. *J. Am. Chem. Soc.* **1984,** *106,* 4625.